



## UvA-DARE (Digital Academic Repository)

### Photonic control over light absorption and emission in photovoltaics

Veeken, T.P.N.

**Publication date**  
2022

[Link to publication](#)

#### **Citation for published version (APA):**

Veeken, T. P. N. (2022). *Photonic control over light absorption and emission in photovoltaics*.

#### **General rights**

It is not permitted to download or to forward/distribute the text or part of it without the consent of the author(s) and/or copyright holder(s), other than for strictly personal, individual use, unless the work is under an open content license (like Creative Commons).

#### **Disclaimer/Complaints regulations**

If you believe that digital publication of certain material infringes any of your rights or (privacy) interests, please let the Library know, stating your reasons. In case of a legitimate complaint, the Library will make the material inaccessible and/or remove it from the website. Please Ask the Library: <https://uba.uva.nl/en/contact>, or a letter to: Library of the University of Amsterdam, Secretariat, Singel 425, 1012 WP Amsterdam, The Netherlands. You will be contacted as soon as possible.

# 1

## Introduction

*“If you don't change direction,  
you will end up where you are heading”*  
— Lao Tzu

Light is at the very heart of life as we know it on earth, as light from the sun heats our planet and provides the energy necessary for animated life forms. The earth is situated at a sweet spot in the solar system, close enough to the sun for the average temperature to be above the freezing point of water and far enough from the sun for the temperature to be below the boiling point of water. For this reason, we have plenty of liquid water on earth, the main ingredient supporting our organic life forms.

Light also has a central role in our perception of the world around us because of our sight. Humans use their eyes in conjunction with their other senses to survive and thrive, though arguably sight is the most versatile of the senses. Across human length scales of millimeters to kilometers, light travels practically instantaneously, providing information at an instant. Our concepts of beauty, color, and vibrancy are due to the astounding capability of our eyes to discern between different wavelengths, intensity, and point of origin of the light it receives. Moreover, we have evolved to interpret the world based on what we see, ranging from discerning edible from inedible food to obtaining social cues through non-verbal communication.

Besides the obvious role light plays in everyday life, light is also central to modern human society. With the advances in electrical lighting, we are no longer bound to the rhythm of day and night for work or social activities. More recently, light also revolutionized our communication and information systems, as it is used as information carrier in optical fibers that serve as the backbone for telecommunication and the internet [1]. Lasers, used for many applications ranging from precise distance measurements to cutting steel, and medical technologies such as endoscopes or optical tomography are also based on light. Finally, optical detection systems continue to revolutionize our world. The first accounts of magnification date back almost 2000 years, and lenses were studied already in the late 1200s [2]. This resulted in the first practical eyeglasses around that time, the first telescopes in the early 17th century, and the development of microscopes by Hooke and Van Leeuwenhoek shortly after

[2]. The consequent development of optical telescopes and microscopes has increased our understanding of the macro and micro parts of our world enormously. Also, over the past few decades, our daily lives have been revolutionized by the advent of photography, personal computers, mobile phones, light-emitting diodes (LEDs), and displays. Even today, research and development of image recognition, optical computing, and biometric sensing continues to shape our future modern world.

Light also plays a key role in the revolution of renewable energy generation. In this thesis, we study how detailed light management can improve the conversion efficiency of sunlight into electricity in photovoltaic cells. Empowered by recent developments in micro- and nanotechnology, we structure materials at the scale of the wavelength to control the flow of light. In this first chapter, we discuss the fundamental properties of light and of energy conversion. We then investigate the potential of solar energy conversion on earth, the fundamental limits of energy conversion by solar cells, and the impressive decrease of the costs of solar power generation over the past decades. The majority of this thesis concerns the use of well-defined nano- or microstructures to control the reflection, transmission, absorption, and emission of light. Therefore, we provide a short overview of the different light management geometries that are commonly used to improve solar cell technologies. We conclude with a motivation and outline of the thesis.

## 1.1 Energy

Light is a form of energy. Textbooks such as ‘The Feynman Lectures on Physics’ teach us about many kinds of energy: “gravitational energy, kinetic energy, heat energy, elastic energy, electrical energy, chemical energy, radiant energy, nuclear energy, mass energy.” [3] Conversion of one type into another type of energy is oftentimes possible but mostly not 100% efficient. Yet, as far as we know, energy is never lost. Energy is a conserved quantity, which means that it is never created nor destroyed. Instead, one type of energy can be converted into a combination of other types while the grand total is constant. It is a simple fact we observe in our universe, but at the same time a marvelous fact — Feynman pointed it out quite cleverly:

*The law is called the conservation of energy. It states that there is a certain quantity, which we call energy, that does not change in the manifold changes which nature undergoes. That is a most abstract idea, because it is a mathematical principle; it says that there is a numerical quantity which does not change when something happens. It is not a description of a mechanism, or anything concrete; it is just a strange fact that we can calculate some number and when we finish watching nature go through her tricks and calculate the number again, it is the same.*

...

*It is important to realize that in physics today, we have no knowledge of what energy is. We do not have a picture that energy comes in little blobs of a definite amount. It is not that way. However, there are formulas for calculating some numerical quantity, and when we add it all together it gives ... always the same number. It is an abstract thing in that it does not tell us the mechanism or the reasons for the various formulas [3].*

Besides different types of energy, we can also discern between sustainable and unsustainable energy sources. Energy from the sun (radiant), wind and hydro (kinetic), and geothermal (heat) are sustainable because they are continuously replenished. In contrast, the use of fossil fuels such as coal, oil, and natural gas (chemical), and nuclear energy are unsustainable; they

can be used only a single time (the time scales for replenishment are orders of magnitude larger than the average human lifetime). Moreover, the fossil fuel industries and the waste produced upon use endanger all forms of life on earth as we know them.

The United Nations list energy as their 7th Sustainable Development Goal (SDG), but recently recognized that practically all other 16 SDGs are linked to energy [4]. For example, Poverty and Hunger (SDGs 1 and 2) can be reduced significantly by access to cheap energy for heating, light, and cooking. Moreover, cheap and clean energy can revolutionize Global Health and access to Clean Water (SDGs 3 and 6), amongst others by providing climate control and water purification. A few other examples are the improvement of Global Education (SDG 4) by internet access, Responsible Consumption and Production (SDG 12) by conversion of traditional to sustainable energy generation, and Decent Work, Sustainable Cities, and Peace (SDGs 8, 11 and 16) by local, independent generation of renewable energy.

Electricity is an important factor in the transition to sustainable energy production and is an important ingredient in our modern living standards. The electrification of global energy use is well underway because of the high conversion efficiency between electricity and other forms of energy, the advances in battery technology, and the increasing use of renewable energy sources. Between 1973 and 2019, the fraction of global energy consumption in the form of electricity rose from 9.5% to 19.7% [5]. However, only 26.5% of that electricity is generated by sustainable energy sources. To meet the global greenhouse gas emission targets, which were agreed upon to limit global warming to well below 2 degrees Celsius compared to pre-industrial levels due to the manifold adverse effects associated with it, we need to replace fossil fuels with renewable energy sources [6, 7]. Solar energy conversion by photovoltaics is one of the renewable energy technologies that is well-suited to replace fossil fuels and has already begun to do so. In the next sections, we will touch upon the tremendous potential of solar energy conversion and the achievements made by photovoltaics until today.

## 1.2 Photovoltaics

The direct conversion of solar light (radiative energy) to electricity (electrical energy) is called photovoltaic energy conversion [8]. A photovoltaic system makes use of the photovoltaic effect: the excitation of an electron from a lower to a higher energy state in a material due to absorption of a photon. Typically, the photovoltaic effect is employed in a semiconductor material, where the photon excites an electron from the valence band (bound state) to the conduction band (unbound state). The energy difference between the highest valence band energy and the lowest conduction band energy is called the bandgap energy (or bandgap in short). An electron can only be excited to the conduction band if the photon has energy equal to or greater than the bandgap. After excitation, the photon's energy has been converted into electric potential energy, stored in the semiconductor material by the separation of the negatively charged electron and the positively charged 'hole' left behind in the valence band.

After a certain amount of time (the 'life-time'), the electron will decay to its initial lower energy state in the valence band, and it has several pathways to get there. A prominent first path is called thermalization: after the electron is excited up into the conduction band, it quickly relaxes to the bottom of the conduction band and transfers its energy to the surrounding atomic lattice in the form of phonons (lattice vibrations; heat). This is one of the reasons that a solar cell heats up when it is illuminated, even though it is designed to convert light into electricity instead of heat. If the electron remains at the bottom of the conduction band, the typical consecutive pathway is called recombination. During recombination, the electron relaxes back to the valence band by recombining with the hole. In the case of radiative

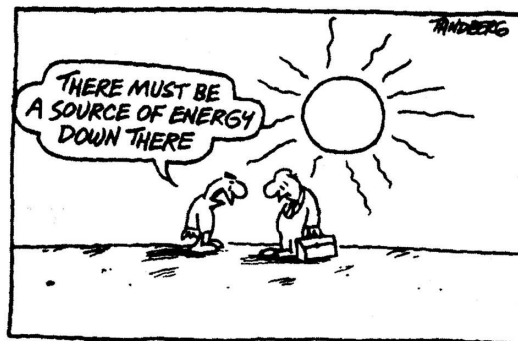
recombination, the electron-hole pair gives up its energy by the emission of a photon with energy equal to the bandgap — this is the mechanism by which a light-emitting diode (LED) generates light. Alternatively, the energy is released as additional heat, in which case we speak of non-radiative recombination. In the case of photovoltaics, we want to convert the chemical potential of the electron-hole pair into an electrical potential before it undergoes recombination. This pathway is enabled by contacting the conduction and valence bands of the semiconductor with electrical contacts. Now, the electron can travel through the contacts back to the valence band and give up its energy in the form of an electrical potential, typically over an electrical resistance between the contacts. The precise engineering of the energy levels in solar cell semiconductor materials and contacts is of tremendous importance to promote the efficient collection of electron-hole pairs [9].

Besides conversion into electricity, solar energy can also be converted into thermal energy, for example, by solar thermal collectors that convert sunlight into hot water. Solar energy is also converted into chemical energy, using either solar photons, solar thermal energy, or solar electricity to produce synthetic fuels (solar fuels). Throughout this thesis, we focus on the improvement of photovoltaic systems. To understand why photovoltaic energy conversion is a candidate for future global-scale renewable energy production, we first look at the potential of solar energy conversion and the fundamental limitations of photovoltaic systems.

### 1.2.1 The potential of solar power

The total amount of solar power received by the earth is astounding. Given the luminosity of the sun and the distance to the earth, we can calculate the intensity of solar light reaching the earth:  $1361 \text{ Wm}^{-2}$ . By multiplying the intensity with the area of the earth as seen from the sun, we obtain the total solar power that reaches the earth: 173 petawatt ( $10^{15} \text{ W}$ )!

A number with this many zero's is quite incomprehensible, so let's put it in perspective. The International Energy Agency (IEA) reports a world total energy supply in 2019 of 606.6 exawatt ( $10^{18} \text{ W}$ ), which corresponds to 19.2 terawatt ( $10^{12} \text{ W}$ ) [5]. That is over 9000 times less than the amount of solar energy received by the earth. In other words, if we could harvest only 0.011% of the solar energy that reaches earth, we would have enough to power the entire planet. Given the nearly inexhaustible power that the sun provides and the fact that it will continue to shine as it does for about another 5 billion years [10], energy from the sun is an ideal source for renewable energy production. In this thesis we study photovoltaic energy conversion of sunlight, however, technically renewable energy sources such as wind, tidal, wave, and hydro energy are also powered by the sun.



## 1.2.2 The spectrum of sunlight

The energy of the sun reaches the earth as electromagnetic radiation, with wavelengths ranging from the ultra-violet (UV) to the visible, near-infrared (NIR), and infrared (IR). Part of that light is reflected back into space by the atmosphere, clouds, and the earth's surface. Another part is absorbed in the atmosphere, thereby heating it, or scattered by atmospheric particles, which explains the typical blue color of the sky and the red color of the sun at sunrise and sunset. Finally, a spectrum of wavelengths reaches the earth's surface, which fluctuates over time due to changes in the atmosphere, the orbit of the earth, and solar activity. For practical analysis purposes, the typical solar spectrum reaching the earth has been standardized as the AM0 (air mass zero) and AM1.5G (air mass 1.5 global) spectra [11]. The AM0 spectrum corresponds to the light that reaches the top of the earth's atmosphere, for which we calculated a total power of  $1361 \text{ Wm}^{-2}$  in the previous section. The AM1.5G spectrum represents the typical irradiance at noon, at an average latitude, clear sky, and including both direct and diffuse illumination. The integrated power is set to  $1000 \text{ Wm}^{-2}$  by definition. Figure 1.1 shows the spectral intensity of the AM1.5G spectrum (black). Most of the intensity is emitted in the visible, 400-700 nanometer (nm), and near-infrared (700-1400 nm) wavelength ranges.

Given the AM1.5G spectrum, we can calculate the maximum power conversion efficiency of a single-junction solar cell, called the detailed-balance (DB) limit [12]. Based on the bandgap of the solar cell and assuming 100% radiative efficiency, the DB model calculates what fraction of the energy in the solar spectrum can be converted to electricity. For a single-junction solar cell, this limit is at 33.7% for a bandgap energy of 1.34 eV ( $\lambda = 925 \text{ nm}$ ) [13]. A silicon solar cell (bandgap 1.12 eV;  $\lambda = 1107 \text{ nm}$ ) has almost the same limit, 33.4%. The fraction of the AM1.5G spectrum that a single-junction silicon solar cell could convert is plotted in Fig. 1.1a in orange. The inset in Figure 1.1a shows a schematic of the semiconductor valence and conduction bands discussed before, with the bandgap that matches the energy of the photon indicated by the green arrow. The elementary charge times the open-circuit voltage,  $qV_{oc}$ , is slightly lower than the bandgap, which we will discuss in the next section. Light with energy below the silicon bandgap cannot be absorbed (red arrow), thus beyond 1107 nm wavelength, the conversion is zero in Fig. 1.1a. Furthermore, light with energy greater than the bandgap excites the valence electron higher up into the conduction band (blue arrow), where it quickly

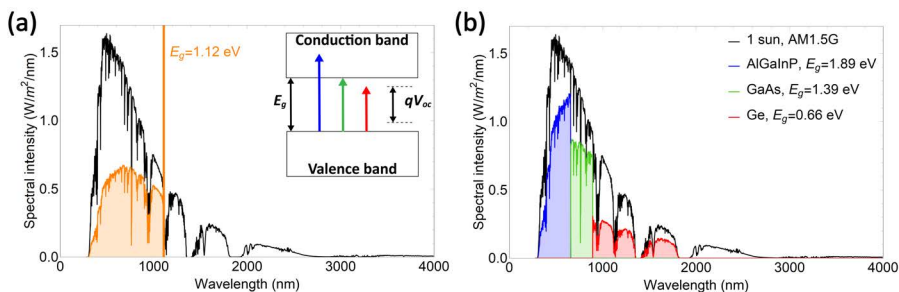


**Figure 1.1:** AM1.5G solar irradiation spectrum (black) and the energy utilization spectrum (a) for an ideal silicon solar cell (bandgap: 1.12 eV, detailed-balance efficiency limit: 33.4%) and (b) for an ideal multi-junction solar cell (bandgaps: 1.89/1.39/0.66 eV, detailed-balance efficiency limit: 51.6%).

thermalizes to the bottom of the conduction band, losing its energy as heat. Thus, photons with a shorter wavelength than 1107 nm do not convert all of their energy in the silicon solar cell — this is the reason that the orange curve is well below the AM1.5G intensity in Fig. 1.1a. A maximum efficiency of 33.7% might seem rather low at first sight, but the typical electricity conversion efficiency of a coal or natural gas power plant in the United States in 2020 was similar: 32% and 44%, respectively [14].

One of the efforts to decrease the losses from thermalization and lack of absorption in a solar cell is the use of two or more absorber materials with different bandgaps in a single device. Such a device is called a multi-junction or tandem solar cell. Each of the subcells efficiently converts the part of the solar spectrum that matches its bandgap. Figure 1.1b shows the DB conversion limit for a triple-junction solar cell made of compound materials AlGaInP and GaAs, and germanium (Ge). Scaling from a single-junction to a triple-junction solar cell increases the DB conversion limit from 33.7% to 51.6%. This increases the potential of photovoltaics tremendously, both for large-scale cost-competitive tandem devices [15] and ultra-high efficiency tandem devices for niche applications such as vehicle-integrated PV [16] or solar power harvesting in space [17] that can permit higher costs.

Many other approaches to solar energy conversion beyond the DB limit are being explored. A notable example is that of bifacial silicon solar cells, which is a typical silicon solar cell with metal wire contacts on the back rather than a full metal contact. This allows light to also enter from the back, adding to the generated power because there is more than ‘1-sun illumination’. This type of solar cell already had a market share of 20% in 2020 and this share is expected to increase up to 70% by 2030 [18]. Another approach is that of multiple exciton generation: exciting multiple low-energy charges with one high-energy photon. Up- and down-conversion of sunlight is also explored, converting a high-energy photon into multiple low-energy photons or vice versa. Limiting the radiative emission angles to raise the output voltage also poses significant potential [19]. Finally, in concentrating photovoltaics, light is focused onto a solar cell to increase its output power. Typically, large-scale optics such as mirrors and lenses are used to increase the solar flux, boosting mainly the current density, which requires direct illumination and actively maintaining orientation towards the sun.

In the next two sections, we summarize the progress that has been made on the power conversion efficiency for several single-junction solar cells. We also address the photovoltaic systems that could exceed the single-junction detailed-balance limit.

### 1.2.3 Detailed-balance solar cell efficiency limit

In Figure 1.1a, we calculated the fraction of the solar spectrum that could be converted for a single material, in this case, silicon with a bandgap at 1.12 eV. If we calculate this fraction for a range of bandgaps, we obtain the black curve plotted in Figure 1.2a: the detailed-balance efficiency limit for bandgaps between 0.5 eV ( $\lambda \approx 2480$  nm) and 1.95 eV ( $\lambda \approx 635$  nm). As we noted before, we find the maximum for a bandgap of 1.34 eV and a second peak around 1.12 eV, marking the trade-off between the absorption of lower-energy photons and the efficient conversion of higher-energy photons. If we decrease the bandgap further, the DB efficiency quickly decreases: although more sunlight can overcome the bandgap energy barrier, more energy is lost due to thermalization (red fraction in Figure 1.1b). If we increase the bandgap beyond 1.34 eV, the DB efficiency also drops: now less energy is lost due to thermalization (blue fraction in Figure 1.1b), but less light is absorbed. The DB efficiency curve marks the ideal bandgap range for photovoltaic energy conversion and allows for comparison between different solar cell types. The semiconductor bandgaps of different materials depend on their building blocks (atoms, molecules, nanocrystals) and their arrangement (crystal, amorphous,

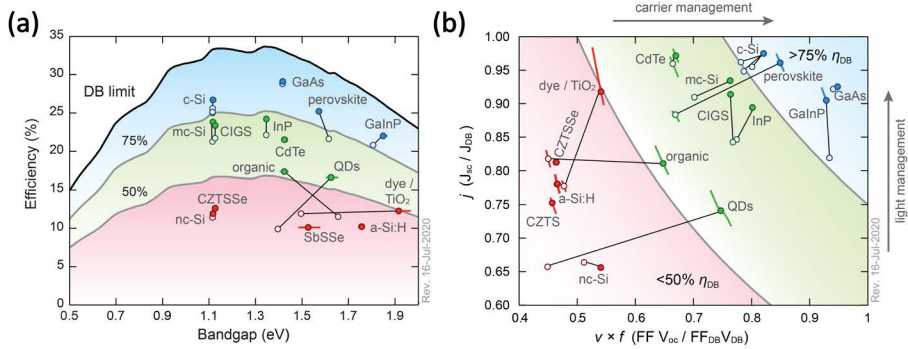


**Figure 1.2: Fraction of the detailed-balance (DB) limit for record-efficiency solar cells of 15 different materials. The open symbols show the record values from April 2016, the solid symbols show the values in July 2020. Figures from references [13] and [20], which are continuously updated with data from new record-efficiency solar cells and made available at <https://www.lmpv.nl/DB/>** (a) Fraction of the DB efficiency limit (black line) as a function of the bandgap. Gray lines show 75% and 50% of the limit. (b) Fraction of the DB current density ( $j$ ) versus the fraction of the DB voltage times fill factor ( $v \times f$ ), corresponding to the efficiencies in panel (a).

host-material, passivation, and spacer layers). As we will see, there is a remarkable breadth of materials with different or even tunable bandgaps and corresponding record efficiencies.

The power conversion efficiency of solar cells has been improved upon for over half a century. In 1954, the first practical solar cell was demonstrated at Bell Labs, a crystalline silicon solar cell with 6% efficiency [21]. A vast global research effort ensured a steady increase in efficiency over time, and in 2017, the newest world-record efficiency for a silicon solar cell was set at 26.7% [22]. Besides silicon, many more material systems have been successfully explored for photovoltaics. Figure 1.2a shows the current world-record efficiencies for 15 of the most commonly used materials, plotted against their bandgap and the DB limit we discussed in the previous section. Over the past several years, we have continuously updated these Figures that were first published in 2016 by Polman et al. [13]. The updated Figures are publicly available at <https://www.lmpv.nl/DB/>.

In 2020, we published the updated Figures in a review paper looking back at the progress over the previous 4 years [20]. The open and closed data points in Figure 1.2a show this progress between 2016-2020, for each material system. The blue, green, and red shaded backgrounds indicate the performance as a fraction of the DB limit, respectively  $>75\%$ ,  $>50\%$ , and  $<50\%$ . Above 75%, we find ultrahigh-efficiency mono-crystalline materials such as Si, GaAs, GaInP, and more recently also perovskite. On the other hand, we see the most impressive efficiency increases for QD and organic solar cells. The plethora of materials used in photovoltaics nowadays and their continued advancement makes for a robust industry, offering many options for many different mainstream and niche applications [15].

There are several reasons why even record solar cells do not come much closer than 75% of the DB limit. We can understand them by looking at the components that make up the generated electrical power at the maximum power point  $P_{mp}$ :

$$P_{mp} = V_{oc} \times J_{sc} \times FF = V_{mp} \times J_{mp}. \quad (1.1)$$

Here,  $V_{oc}$  is the open-circuit voltage, the output voltage of the solar cell when the circuit is not closed: the electrical resistance is infinite and no current flows.  $J_{sc}$  is the short-circuit current density, the current that the solar cell generates when the electrical resistance is zero, and thus, the voltage is zero. Finally, FF is the fill factor, which accounts for all nonidealities in the cell. Expressed as  $FF = (V_{mp}J_{mp})/(V_{oc}J_{sc})$ , the FF indicates how well the voltage and current density approach their maximum values at the maximum power point. Fundamentally, the FF cannot become unity because the resistance in the circuit cannot be zero (short-circuit) and infinite (open-circuit) at the same time. Moreover, a finite load is needed to harvest the energy because both  $V$  and  $J$  need to be nonzero for the power ( $P$ ) to be nonzero.  $V_{mp}$  and  $J_{mp}$  are defined as the voltage and current density that together generate the maximum amount of power and stipulate the ideal electrical resistance in the circuit. With the specified maximum generated power, we can calculate the efficiency of the solar cell according to:

$$\eta = \frac{P_{mp}}{P_{AM1.5G}}, \quad (1.2)$$

with  $\eta$  the power conversion efficiency and  $P_{AM1.5G}$  the power in the AM1.5G solar spectrum, which is defined as  $1000 \text{ Wm}^{-2}$ .

Now that we have separated the voltage and current density components in the generated power, we can specify the implications of a few notable nonidealities in a solar cell. First and foremost, a realistic solar cell does not absorb all incident sunlight in the active layer. Instead, fractions of the light are lost due to reflection, incomplete absorption, or parasitic absorption in other layers, which lowers the generation rate of carriers (electron-hole pairs). This mainly lowers the  $J_{sc}$ . Incomplete collection of the generated carriers can further lower the  $J_{sc}$ . The  $V_{oc}$  is decreased by phenomena such as Auger recombination, band tail recombination, and recombination in the bulk, and at interfaces and surface defects [13]. Finally, nonidealities such as electrical resistance and contact losses are captured in the FF. Combined, these are the reasons why the record-efficiency solar cells in Figure 1.2 are below the DB limit.

Figure 1.2b shows the fraction of the DB limit of the voltage, FF, and current density according to Equation (1.1), corresponding to the record efficiencies shown in Figure 1.2a. As discussed in the previous paragraph, now we can understand that the current density axis indicates to what degree the light management is the limiting factor (incomplete absorption), while the voltage  $\times$  FF axis indicates the limitation by charge carrier management (recombination). Interestingly, the ultrahigh-efficiency materials show either near-perfect light management (Si and perovskite) or near-perfect carrier management (GaAs and GaInP). Similarly, the CIGS and dye records advanced mainly by increased light management, while the organic and QD records advanced mostly by improved carrier management. This indicates that both light management and carrier management are very active areas of photovoltaics research and development.

Improving carrier management requires understanding and control over the recombination mechanisms in a solar cell [13]. This is mostly a materials science challenge, with a focus on the quality of materials and interfaces. The focus of this thesis is on the improvement of light management, which requires control over the propagation and absorption of light inside the cell. Although light management also benefits from material quality, the main challenge is to achieve absorption in the active layer. It is a dynamic game, where the goal is to simultaneously reduce the reflection, transmission, and parasitic absorption of light with energies above the solar cell bandgap, and decrease heating from below-bandgap light. Photonic concepts offer a plethora of possible light management techniques for several different applications. The bulk of this thesis is concerned with *photonics for photovoltaics*, so in the next section we will explore this field of study in more detail.

## 1.3 Photonics for photovoltaics

Light is an amazing phenomenon. We understand it as a quantized packet of energy that has a momentum but no mass and can therefore travel at the maximum speed in our universe — the speed of light. As we describe light in more detail, we find that it behaves either as a particle or as a wave, depending on its environment: the famous particle-wave duality. In the particle description, light behaves like objects we know from ordinary life: a ball will either bounce back from a solid wall or move through a hole in that wall. Similarly, a light particle, called a photon, will reflect from a mirror or transmit through a hole in that mirror. The analogy is almost perfect, except for the fact that a photon has a probability associated with reflection, transmission, or absorption by a material, while the ball will bounce from the wall with 100% certainty. Thus, even in the particle description of light, we describe the propagation of a photon with probabilities (relating to the quantum mechanic nature of light). When we have a large number of photons, for instance, when we measure the number of photons reflected by and transmitted through a window, we find back the probabilities in the statistics of reflected or transmitted photons. When the features of the environment are much larger than the wavelength of the light, we can model light with geometric (ray) optics. This model, which we use in **Chapters 3 and 6**, describes light propagation as rays moving in straight lines that behave according to the statistics described before. However, to explain the full behavior of light, we have to describe it as a wave.

In the wave description, light behaves much like a wave on the ocean: it has a certain distance between the tops (called the wavelength), travels at a certain speed, and the amplitude of the wave can be interpreted as the number of photons. In contrast to the particle description, we can describe the phenomenon of light interference in the wave description. In daily life, we know of the interference of water waves, for example, when we throw two stones next to each other in a pond: each stone creates a circular water wave by its impact. When the two waves meet, they interfere: crests in the waves add up to higher peaks; troughs in the waves add up to lower depths; and a crest and a trough dampen each other. Effects such as interference become dominant when we shrink down the material that we illuminate down to the size of the wavelength. For visible light, the wavelength lies roughly between 400 and 700 nm (ultraviolet - red), which corresponds to 0.0004 - 0.0007 millimeter (mm). When we talk about nanotechnology or the nanoscale, we refer to materials with features with this length scale and smaller (1 - 1000 nm). Nanoscale materials have been used for centuries because of their special interaction with light, for example, the use of gold nanoparticles that cause the colors in stained glass windows and the famous Lycurgus Cup [23]. However, the advances made over the past few decades in micro- and nanoscale fabrication, (nano)photonic light management, and powerful electromagnetic simulation methods have sparked a rich field of research on photonic light management.

### 1.3.1 Photonic light management

Typically, light travels in straight lines and undergoes reflection, transmission, refraction, and absorption when it interacts with a material. The strength of reflection and refraction at an interface is dictated by the refractive index of the materials. The imaginary part of the refractive index, the extinction coefficient, dictates the absorption of light in a material (Beer-Lambert law) and thereby the transmission. For a high-efficiency solar cell, the challenge is to maximize the absorption of light in the active layer (the semiconductor layer where charges can be extracted). This implies that the reflection of incident light must be minimized, and all other layers must transmit the light to be absorbed in the active layer. To absorb all the light, the active layer of a conventional solar cell must be ‘optically thick’. Because the strength of the extinction coefficient varies strongly between different semiconductor materials, this thickness varies from a few micrometers ( $\mu\text{m}$ ) for direct-bandgap materials such as gallium arsenide (GaAs) to several hundreds of micrometers for indirect-bandgap materials such as Si. A large optical thickness poses a dilemma for conventional solar cells because the use of a thicker solar cell increases light absorption but also increases the losses in extraction and recombination. Photonic design can help increase the absorption of incident light, thereby enabling the use of a thinner solar cell.

For a silicon solar cell, incident light experiences a large contrast of refractive index at the air-silicon interface of about a factor 4. This impedance mismatch for an electromagnetic wave traveling in air or silicon causes strong reflection at the interface (given by Snell’s law). This mismatch can be reduced by placing a material in between the air and silicon that has a refractive index between that of air and silicon. A commercial solar cell has several of these materials, such as the silica module glass, a transparent conductive oxide (TCO) contact, and/or an anti-reflection layer such as silicon nitride ( $\text{Si}_3\text{N}_4$ ). Alternatively, nanoscale structuring of the material can also reduce reflection. In the simplest case, the structuring is much smaller than the wavelength, such that the light propagates as if it was in a single material with an effective refractive index. The validity of this effective medium approximation is discussed in **Chapter 6**. Figure 1.3a shows this effect in a schematic: the top surface of the solar cell (light blue) is structured to enhance light propagation into the solar cell.

When we increase the size of the features on top of the solar cell in Figure 1.3a to the scale of the wavelength, we enter a regime of resonant light-matter interaction. In this case, the interaction is enhanced because the wavelength matches the length scale of the material and the energy of light is temporarily stored inside the nanostructure. In daily life, we know this effect from the sound of a guitar string (the wavelength matches the length and material of the string) or from the tuning of a radio (the radio antenna resonates at the radio frequency).

When light interacts with a material that is structured at the nanoscale, this can cause several resonant effects, depending on the material properties, such as Fabry-Pérot constructive or destructive interference [24], or the coupling to Mie-like resonances (dipolar or multipolar polarization of the material) [24–26], plasmon resonances (localized excitations or propagating modes on the surface of a metal) [27], or waveguide modes (propagation confined to one or two dimensions) [28].

Fabry-Pérot type resonances were discussed above as the typical flat, thin-film anti-reflection layers of a solar cell. Mie-like resonances are discussed in detail in **Chapter 2**. In Figure 1.3, Mie-like resonances in panel (a) cause forward scattering of light under an enhanced angular range into the solar cell to achieve light-trapping. In Figure 1.3(b), Mie-like resonators are designed for infrared light to achieve enhanced cooling of the cell — this concept of passive radiative cooling is discussed in **Chapter 5**. In panels (c), (e), and (f), Mie-like resonators are used to control the reflection and transmission of light at interfaces

depending on their wavelength. In panel (c), high-energy light is reflected back into the top subcell of a tandem solar cell, while low-energy light is transmitted into the bottom cell. In panel (f), the same effect is pursued and dynamically adapts to the performance of the subcells (for example, to improve current-matching). In panel (e), light of a specific wavelength is reflected to “color” a solar cell (structural color), while most light is transmitted into the cell for conversion (not drawn). Panel (d) shows the effects of up- or down-conversion of light, as discussed earlier. In down-conversion, high-energy photons (blue) are converted into multiple low-energy photons (red), which reduces thermalization losses; up-conversion does the inverse, enabling conversion of light with energy below the bandgap. These types of conversion are achieved by absorption and subsequent emission of light — control over these processes with nanophotonic structures is discussed in **Chapters 2 and 4**.

The concepts of light management in photovoltaics were first explored with plasmonic resonances, as reviewed in references [27, 29]. It was found that parasitic absorption caused by the metal building blocks made the use of plasmonics in solar cells challenging. Many of the concepts first shown with plasmonics were then pursued with all-dielectric nanophotonic resonances such as those discussed above [13, 30–32]. In this thesis, we focus on the use of all-dielectric nanostructures that can be used to enhance photovoltaic energy conversion.

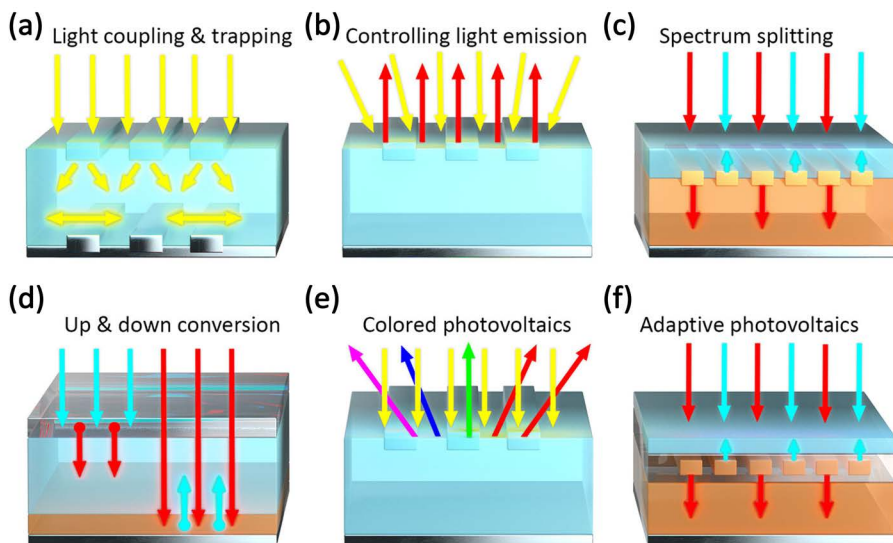


**Figure 1.3:** Schematic of photonic light management geometries to optimize photovoltaics. Figure from ref. [32].

## 1.4 Motivation

In the previous sections, we have seen that an enormous amount of solar energy reaches the earth, that photovoltaics is a mature technology that can convert this energy to electricity, and that photonics can improve both conventional and new types of photovoltaic systems. Yet, even after decades of research and technological advancements, there are two key challenges that remain to be overcome. The first is to further reduce the cost of solar electricity generation to enable it as one of our main energy sources, and the second is the integration of solar electricity generation into buildings, landscapes, and infrastructures. We briefly discuss them both as the motivation to this thesis.

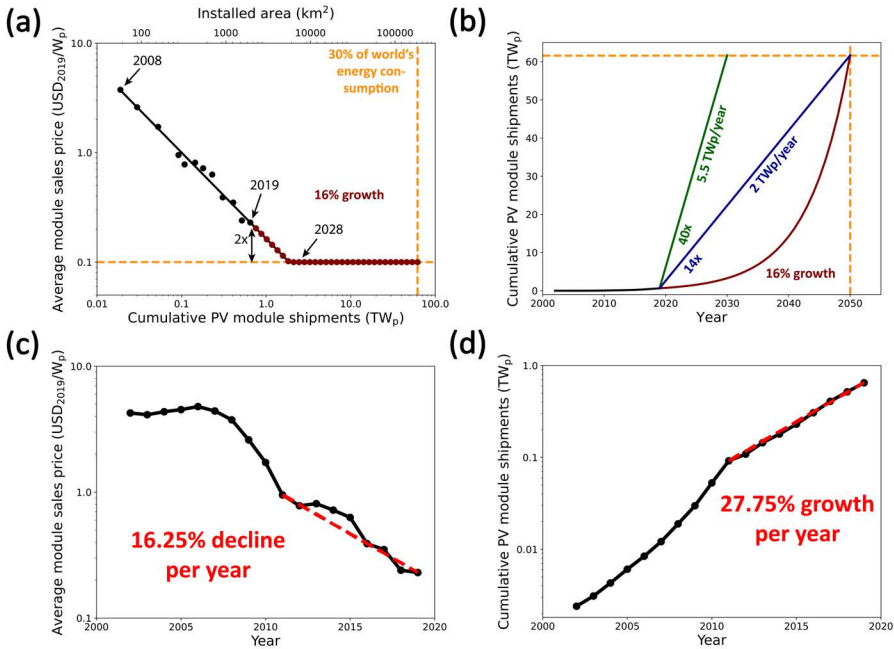


**Figure 1.4: Cost reduction and PV installation growth.** (a) Average sales price of Si solar modules normalized by the generated power under standardized conditions ( $W_p$ ) as a function of total installed capacity since 2008. Data from the ITRPV report [18]. Red data points are extrapolations of the 22% annual cost reduction at a yearly 16% growth of installed capacity, assuming that module prices will saturate at a price of 0.1 US\$/W<sub>p</sub>. (b) Historic realization (black) and 16% annual fixed growth scenario (red) of installed PV capacity. The linear curves correspond to increased PV installation rates (14/40× compared to ~0.1 TW<sub>p</sub>/year in 2019, to reach a 60 TW<sub>p</sub> target in 2050/2030). Panels (a) and (b) from ref. [32]. Panels (c) and (d) plot the historic data of the average module sales price and the cumulative module shipments, respectively, versus the corresponding years (2002-2019). It shows essentially the same data as the black lines in panels (a) and (b) but visualizes the exponential decline in price over time and the simultaneous exponential growth of the installed capacity over time.

Given the disparity between a finite amount of fossil fuels and near-infinite solar energy supply, one might conclude that solar is an obvious choice and bound to replace fossil fuels. Yet, even by the year 2040, fossil fuels are expected to still supply more than half our global energy supply [5]. The fossil fuel industry supplies many jobs and is a key economic driving force of our modern society, but most of all it supplies very inexpensive energy. Where (global) policy can surely impact the transition to renewable energy use, lowering the cost of PV-generated power will certainly accelerate the transition. Figure 1.4a shows the historic price data from 2008 until 2019 in black: the average module sales price vs. the cumulative PV module shipments (global installed area). The curve shows an exponential decline in the average price (Fig. 1.4c) and an exponential increase in the installed area (Fig. 1.4d). This power law relation is very impressive, sustaining an installed-capacity growth of 16% per year, mainly fueled by economy of scale as the production capacity increases [13]. In Figure 1.4a, Garnett et al. assumed a saturation at a price of 0.1 dollar (USD) per watt-peak ( $W_p$ ). This is a fair assumption for the current market that is dominated by silicon technology, where the costs of the raw materials of the cell and module cannot scale down forever. If we could sustain this 16% growth until the year 2050 (red dots), this would yield an estimated 30% share in the world energy consumption ( $\sim 60 \text{ TW}_p$  installed capacity). Here, we assume the global primary energy supply would grow from 18 TW in 2019 to 23.5 TW in 2050 [33]. To generate an average of 7.05 TW (30% of 23.5 TW) with PV, assuming a global PV capacity factor of 8.5, we obtain the estimated  $\sim 60 \text{ TW}_p$  installed capacity.

However, such exponential growth of the installed capacity has the most impact in the final years, as is clearly visible in Figure 1.4b: the black line is the historic installed capacity on a linear scale; the red line the projected exponential increase at 16% per year. In the exponential projection, only about a quarter of the  $\sim 60 \text{ TW}_p$  is installed by the year 2040. Alternatively, also two linear projections are plotted that start in 2019, which need an abrupt  $14/40\times$  increase in the added module shipments per year, and need to sustain that pace until 2030/2040. Evidently, the linear cases will not be met, but it does demonstrate the upscaling of the solar panel manufacturing that is needed. Polman et al. have put in perspective how much area actually would be needed to power the world with solar energy only, indicating that it is not impossible:

*“Assuming a modest module efficiency of 20%, a system capacity factor of 15%, an average ground cover ratio of 50%, and 50% losses related to storage and secondary conversion, 1.6% of Earth’s land area would be required to produce an amount of energy equal to the current primary supply (18 TW in 2019). Although in absolute terms this is a very large number, it is not unrealistic. To put this in perspective, this area is less than 5% of the area used for agriculture worldwide. Also, note that substantial land areas are already used today for production of fossil fuels and various types of biofuel. Finally, by drastically increasing the efficiency of solar modules, by integrating PV into buildings and other objects, and by combining PV technology with other renewable sources such as solar thermal energy and wind energy, a much smaller land area would be needed.” [13]*

To power our world with clean, renewable, and at least climate-neutral energy, we need to replace fossil fuels, with solar energy playing a major role. To meet the global greenhouse gas emission targets [6, 7], we have to accelerate the energy transition beyond the current exponential growth. This can be done by making solar modules even cheaper. This can mean either producing the same module at a lower price or producing a higher-efficiency module at the same price, which indicates the need for further research and development of PV. However, accelerating the growth can also be achieved by producing entirely different types of PV: for

example, by producing flexible, thin-film PV at half the efficiency but more than two times cheaper, or a tandem device at the same price but higher efficiency. These technologies are not commercially available yet but are potentially disruptive.

The second challenge, the integration of solar electricity generation into the environment, concerns where we install different kinds of PV systems. Solar power plants typically deploy high-efficiency, flat panel solar modules covering large land areas. Especially countries with high population densities, such as The Netherlands, necessitate the further development of high-efficiency PV in landscapes. The use of PV with somewhat lower efficiency (e.g., 15-20%) at a very low cost might be a viable option for certain cases or regions that are not limited by the physical area. Complementary to installing PV in landscapes, it can be installed in buildings and infrastructures. Building-integrated photovoltaics (BIPV) covers many different types of PV technologies, ranging from conventional silicon solar cells integrated into roofs [34] or walls [35], colorful solar cells [36, 37], or even semi-transparent PV. In **Chapters 3 and 4**, we present our efforts to enhance the efficiency of luminescent solar concentrators as semi-transparent BIPV. Photonic concepts are particularly important for these emerging types of PV, for example, to engineer the color of the photovoltaic, ensure light trapping in thin, lightweight, and flexible PV, or combine semi-transparency with efficient power generation in windows.

To conclude this motivation, we take a look at the estimated area of PV we would need in the Netherlands to generate 50% of the primary energy consumption in 2019. Here, we consider a typical solar panel of  $300 \text{ W}_p$  per  $1.5 \text{ m}^2$ , the solar capacity factor in the Netherlands of 11.3, and the energy consumption of 0.13 TW, both in 2019. Figure 1.5 shows the estimated area of  $60 \times 60 = 3600 \text{ km}^2$ , almost 9% of the land area of the country, amounting to  $\sim 735 \text{ GW}_p$  installed PV capacity. As mentioned before, it might be impossible to cover 9% of the land area with PV. Estimating the installation of PV in landscapes to be limited to 3%, we have a need for large-scale integration of PV into buildings, infrastructure, and possibly even PV on water. The necessary area also decreases by increasing the efficiency of the PV; in **Chapters 5, 6, and 7**, we investigate the use of radiative cooling and the reduction of reflection losses to increase the efficiency of solar cells.



**Figure 1.5:** Map of the The Netherlands. The yellow square indicates the area needed for photovoltaics to power 50% of the estimated primary energy consumption of the Netherlands in the year 2050.

## 1.5 Outline of the thesis

The absorption and emission of light can be controlled using photonic structures. In the first part of this thesis, we investigate the use of resonant nanophotonic structures to control the angular distribution of luminophore emission (quantum dots or nanoplatelets). In the second part of the thesis, we investigate the use of micro- and nanostructures in silicon solar cells to enhance infrared emission for radiative cooling and to reduce reflection of visible and near-infrared light.

### Part I: resonant nanophotonic structures for directional emission

In **Chapter 2**, we present a soft-stamping method to selectively print a homogeneous layer of CdSeTe/ZnS core-shell quantum dots (QDs) on top of an array of Si nanocylinders with Mie-type resonant modes. Using this new method, we gain control of the QD's angular emission through engineered coupling of the QDs to these resonant modes. We show enhanced upward or downward QD emission depending on the cylinder size, as well as enhanced absorption of laser light due to the cylinder array.

In **Chapter 3**, we employ Monte Carlo ray-trace modeling to evaluate the conversion efficiency of luminescent solar concentrators (LSC) using anisotropic luminophore emission as a function of photoluminescence quantum yield, waveguide concentration, and geometric gain. By spanning the full LSC parameter space, we define a roadmap towards high LSC conversion efficiency. An analytical function is derived for the dark radiative current of an LSC to calculate the conversion efficiency from ray-tracing results. We provide design parameters for optimized luminescent solar concentrators with practical geometrical gains of 10. Using luminophores with strongly anisotropic emission and high (99%) quantum yield, we conclude that conversion efficiencies beyond 28% are achievable.

In **Chapter 4**, we demonstrate anisotropic luminophore emission that can be used to enhance light trapping in the LSC waveguide. By embedding semiconductor nanoplatelet emitters into high-index TiO<sub>2</sub> nanocylinders, we alter their angular emission profile to increase emission into total internal reflection (TIR) angles. The emission direction can be controlled by tweaking Mie-like multipolar resonances in the individual nanocylinders (form factor) and the interaction with the lattice (structure factor). Angle-resolved photoluminescence measurements on the fabricated nanocylinders arrays corroborate this understanding. By optimizing the cylinder shape and lattice spacing, we show an increase in light trapping from 75% (isotropic emission) to 83.5%.

### Part II: resonant nanophotonic structures for directional emission

In **Chapter 5**, we investigate the use of passive radiative cooling (PRC) to dissipate excess heat from a solar cell into or through the earth's atmosphere. For a silicon solar cell, the challenge is to enhance PRC while simultaneously retaining transparency for sunlight above the silicon bandgap. We fabricate a hexagonal array of microcylinders that can be integrated on top of the solar cell module glass. We show very good comparison between simulations and measurements of the infrared spectra while retaining transparency for above-bandgap light.

Textured silicon solar cells that achieve ultra-low reflectance are called black silicon (BSi) because of their black appearance. The diversity and complex surface structures of BSi make it challenging to commercialize BSi devices. Modeling and simulation are commonly used in the semiconductor industry to better understand the material properties, predict the device performance, and provide guidelines for optimizing fabrication parameters. In **Chapter 6**,

we model three BSi nanotextures, each with a distinct random geometry, with an effective medium approximation (EMA). We validate the use of EMA with full-wave optical simulations. We propose criteria for the validity of different optical simulation techniques for a set of industrial photovoltaic textures. This analysis reveals a region within which neither geometric optics nor EMA are adequate for calculating the reflectivity of a textured surface, and hence full-wave optical simulations are required.

Finally, in **Chapter 7**, we investigate the accurate characterization of BSi textures. We compare 3D models of challenging BSi textures obtained by atomic force microscopy (AFM) and plasma focused ion beam (PFIB) tomography techniques. Hemispherical reflection measurement results are compared to full-wave optical simulated results to test the reliability and consistency of the tomography models. Our results provide strong evidence that PFIB tomography is a better substitute to the AFM for highly roughened surface topographical characterization such as BSi, which provides surface 3D models with better reliability and consistency.

Overall, this thesis provides new insights into multiple light management strategies to improve photovoltaic systems. Many of these insights are more generally applicable to other optoelectronic devices, including photodetectors, light-emitting diodes, and displays.